

Towards Automatic Robotic NDT Dense Mapping for Pipeline Integrity Inspection

Jaime Valls Miro, Dave Hunt, Nalika Ulapane and Michael Behrens

Abstract This paper addresses automated mapping of the remaining wall thickness of metallic pipelines in the field by means of an inspection robot equipped with Non-Destructive Testing (NDT) sensing. Set in the context of condition assessment of critical infrastructure, the integrity of arbitrary sections in the conduit is derived with a bespoke robot kinematic configuration that allows dense pipe wall thickness discrimination in circumferential and longitudinal direction via NDT sensing with guaranteed sensing lift-off (offset of the sensor from pipe wall) to the pipe wall, an essential barrier to overcome in cement-lined water pipelines. The data gathered represents not only a visual understanding of the condition of the pipe for asset managers, but also constitutes a quantitative input to a remaining-life calculation that defines the likelihood of the pipeline for future renewal or repair. Results are presented from deployment of the robotic device on a series of pipeline inspections which demonstrate the feasibility of the device and sensing configuration to provide meaningful 2.5D geometric maps.

1 Motivation - A Taxonomy of NDT Inspection Techniques

Non-Destructive Testing (NDT) or Evaluation (NDE) is extensively employed by the energy and water industry to assess the integrity of their network assets, particularly their larger and most critical conduits (generally referred to as those larger than 350 mm in diameter), in their decision-making process leading their renewal/repair/rehabilitation programs. The key advantage of NDT/NDE is that the structure of the asset is not compromised in estimating its condition.

The sensing modality to use is strongly influenced by the material of the asset. Grey Cast Iron (CI) pipelines remain the bulk of the buried critical water infras-

Jaime Valls Miro, Dave Hunt and Nalika Ulapane
Centre for Autonomous Systems, University of Technology Sydney,
e-mail: {jaime.vallsmiro,dave.hunt,nalika.ulapane,michael.behrens}@uts.edu.au

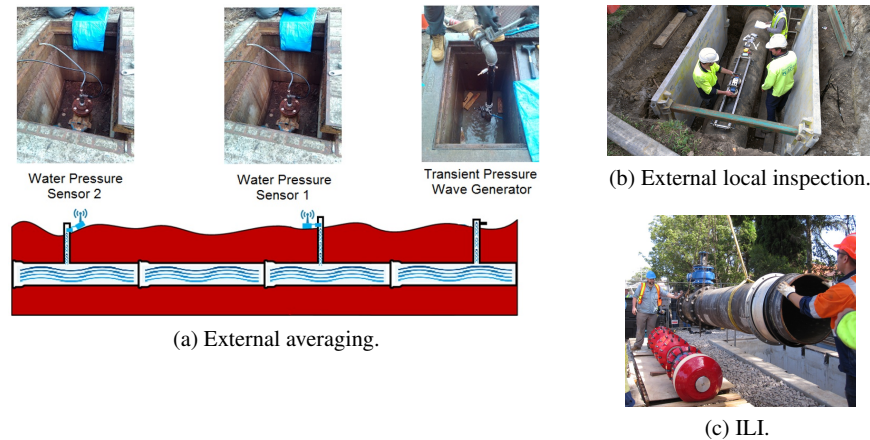


Fig. 1: Example of various configurations of NDT tools.

structure in the developed world as that was the material of choice for mass production with the advent of the Industrial Revolution in the middle of the 18th century (alongside its less brittle relative of Ductile Iron since the nineteen fifties), until carbon steel, asbestos cement or plastic pipelines (PVC) amongst other materials made them redundant over the years. The non-homogeneity of the CI produce means that sensing techniques widely employed in the (mild) Carbon Steel networks in the energy pipeline sector, such as ultrasonics or electromagnetic acoustic transducers (EMAT), are inadequate for CI, and the underlying techniques of most commercial propositions for CI are instead based on either magnetics (e.g. Magnetic Flux Leakage (MFL), Pulsed Eddy Currents (PEC) and Remote Field Eddy Currents (RFEC)), or the study of the propagation of pressure waves in the pipeline and/or fluid.

NDT techniques produce results that tend to be a trade-off between deployment costs and information gain. Local inspection techniques (i.e. 1 to 3 meters) can provide dense measurements but are time-consuming and generally costly per unit-length as significant preparatory civil works are required (excavations, network re-routing for guaranteed supply, traffic control, etc). Moreover inspections can only be undertaken at locations which are accessible from the surface. An example of these tools can be seen in Fig. 1b.

On the other hand, the taxonomy of long-coverage tools can be broadly split into techniques that provide average pipe wall measurements over longer distances (generally from a few to 100s of meters, even kilometers), and in-line intrusive (ILI) devices ("smart pigs") deployed inside the pipeline to inspect in higher detail over longer distances (generally 100's of meters to kilometers to make it more cost-effective), while propelled by the operating pressure of the fluid.

The former are generally deployed by accessing the external pipe wall or water column at a few access points spread over the length of the pipeline, either through small key-hole excavations or through external access points such as valves or hydrants. As such they tend to have low or no impact in the continuing operation of the pipeline and are more affordable alternatives for condition assessment. An example can be seen in Fig. 1a. However given the averaging nature of their results, these tools are aimed at providing an initial screening of the condition of an asset, and lack the ability to provide the type of detailed geometry information needed to ascertain likelihood of pipe failure.

Flow-driven ILI tools, on the other hand, are inserted into the charged water column either through standard large appurtenances present in critical mains, or more often than not via dedicated launch and retrieval mechanisms, as depicted in Fig. 1c. While these tools are able to provide direct measurements related to the pipe wall condition over long distances, they do so at the expense of higher disruption to the utilities and combined costs from the substantial civil engineering support from the utility prior, during and post inspection. Moreover, the effectiveness of these techniques has not been fully established within the industry given the consequential validation investment required to do so in a statistically meaningful way.

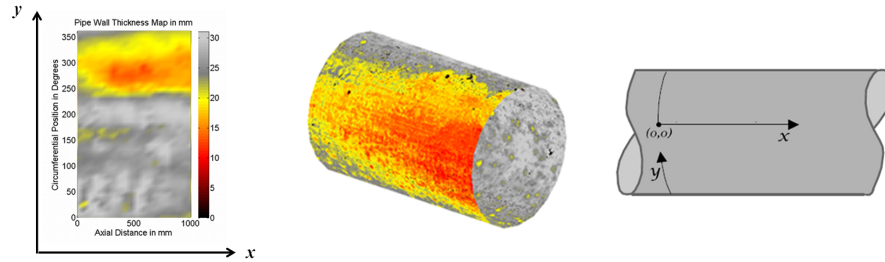
ILI tools present additional shortcomings in the pursuit of attaining an accurate depictions of the condition of a pipe wall:

- they are at the mercy of the pressure of the fluid driving them (both in the tethered and free-flowing case).
- should the tools were to be operated in de-watered conditions, they necessitate complicated winch mechanisms between entry and exit points.
- operating parameters need to be closely controlled (e.g. tool velocity), meaning that discriminating flow controls need to be in place, not necessarily an easy feat to achieve in a complex interconnected network.
- they lack the ability to do fine control and adjustments for mapping (e.g. ensuring tight tolerances in sensor lift-off, repeatability, rectify missed measurements).

Driven by the needs of the water industry the work hereby presented describes the development and field testing of a novel internal NDT inspection robotic vehicle able to:

1. undertake localised, controlled inspections.
2. generate dense NDT mapping suitable for condition assessment and failure prediction.
3. tightly control inherent lift-off during sensing (as induced by the presence of non-magnetic cement lining and pipeline wall irregularities)
4. access arbitrary (within tethered range) pipeline spools from a single point of entry, hence reducing costs to utilities and allowing inspection of inaccessible sections from the surface (e.g. under a rail pass) and minimising disruption to customers (e.g. a pipeline under a driveway).

While the proposed solution requires pipes to be de-watered for deployment, this serves a clear mandate from the utility sector that necessitates a robotic NDT



(a) 2.5D thickness map. (b) Rolled pipe thickness map. (c) Coordinate system on pipe.
 Fig. 2: Axial x and circumferential y coordinates of a 2.5D pipe thickness map.

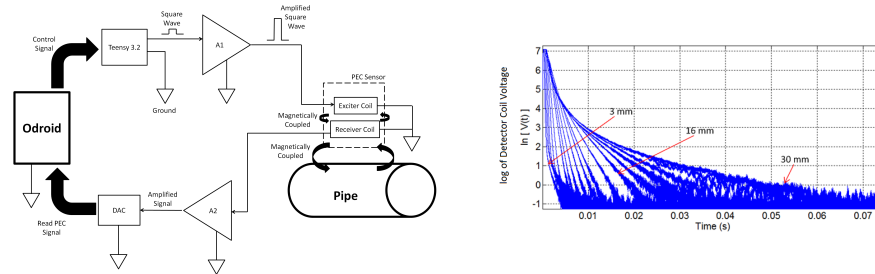
inspection vehicle that can be deployed in an opportunistic manner to ascertain the condition of a particular pipeline, specifically when a mains break occurs, or on the back of a valve inspection or repair program when pipelines are inevitably taken off-line. The remainder of this paper describes such an NDT robot for the inspection of buried network infrastructure and the novelties behind its inception.

2 NDT Pipeline Wall Inspection

Recent research in the space of stress analysis and failure prediction of critical CI water mains has revealed that over and above pit depths, as traditionally provided during condition assessment of a critical asset, there is a need to ascertain the presence and geometries of large corrosion patches in the pipe walls [1], such as those depicted in Fig 12d. There exist a wide range of NDT technologies developed for the purpose of material characterisation for CI [2], yet the provision to build dense 2.5D maps of remaining wall geometries for lined water mains has driven the need to design an internal inspection tool around Pulsed Eddy Current (PEC) sensing technology, as a proven technique typically used in the NDT sector for ferromagnetic material *thickness* estimation [3, 4], resilient to sensor lift-off.

Fig. 2 enables interpreting 2.5D maps of remaining wall thickness produced through PEC sensing, and the conventions shown in Fig. 2 hold for all thickness maps presented herein. The axial location indicates the distance along the pipe's longitudinal axis, while the circumferential location represents rotational degrees around the pipeline. 0° and 360° coincide on the top (crown) of the pipe. In the field inspection results presented in Section 4, longitudinal locations are in reference to the origin set at the robot's entry point to the pipe. The colour bar to the right of the thickness maps is a legend representing thickness in mm, between 0 and 30.

Developed PEC Sensing System A typical PEC sensing system developed for ferromagnetic materials consist of an exciter coil, a detector coil, a voltage pulse generator for excitation and an amplifier for the detected signal. A block diagram of the PEC sensing set up developed for this work is shown in Fig. 3a. Given the size of



(a) PEC sensing operating diagram.

(b) Typical PEC signals on CI thicknesses.

Fig. 3: PEC sensing setup embedded in inspection robot, and typical PEC signals.

the pipes of interest the footprint of the sensor used was 50 mm, indicating that it measures the average thickness of a 50 mm \times 50 mm area under the sensor. Signals captured from the system on different CI thicknesses are shown in Fig. 3b and as reported in the literature features can be extracted from such signals which can be directly linked to material thickness [5, 6].

Validation of PEC Robot Sensor Setup The validity of the sensor arrangement was first assessed by comparing results on the exhumed CI pipe in Fig. 4 with intact cement lining. The objective was to evaluate how well the measurements agree if a section of the pipe is scanned externally and internally via cement lining. External measurements were performed on known locations with the aid of the grid pattern marked in Fig. 4a. The same locations were scanned internally as shown in Fig. 4b with the aid of the robot localized with reference to the pipe's edge. Measurements were recorded at 50 mm distance increments along rings in the circumferential direction, whilst distance between consecutive rings was set to 100 mm to speed-up the inspection process, since thus generated thickness maps can be then upsampled with minimal information loss as shown in Fig. 12d. The rationale and methodology for this will be further elaborated on in the following two Sections. Strong agreement between both measurements was notable as depicted in Fig. 5; the error histogram in Fig. 5e, calculated by subtracting internal thickness estimates from



(a) Exhumed pipe on which internal and external measurements were performed.



(b) Pipe assessment robot performing internal measurements.

Fig. 4: Laboratory setup with exhumed pipe for internal and external PEC validation.

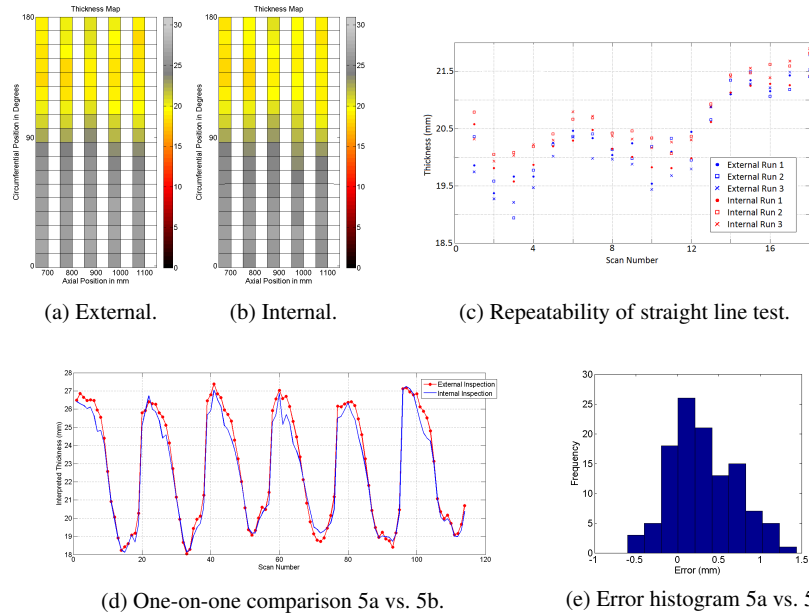
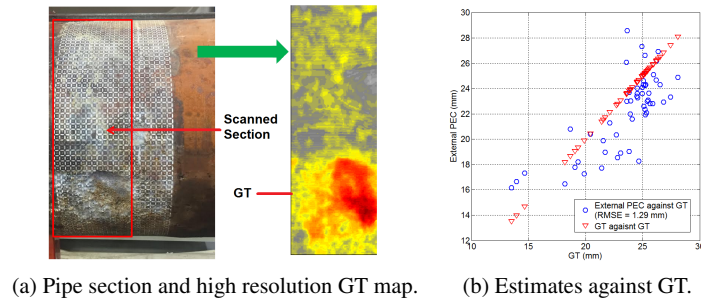


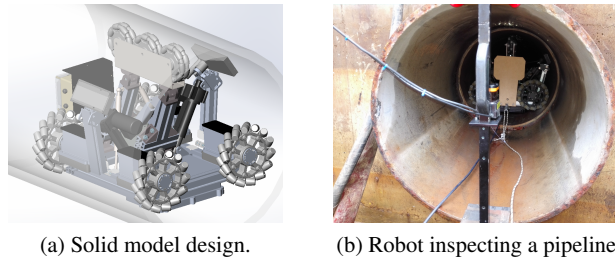
Fig. 5: Thickness maps from internal and external measurements.

external ones hints at a small positive bias in the error, with a mean and standard deviation of 0.323 mm and 0.417 mm respectively. This is an expected result since marginally better sensitivity can be expected when scanning externally (particularly for higher thickness), as the sensor touching the pipe wall can achieving stronger penetration than from the inside given the lift-off effect induced form the cement lining layer. The errors are indicative of acceptable agreement between internal and external measurements confirming the sensor’s suitability for internal assessment of pipes via cement lining. In another sensor verification experiment, Fig. 5c shows results of a repeatability test carried by measuring a straight line along the pipe six times (three times internally and three times externally, with each line having 18 measurements); the average variation on a location was less than 1 mm, indicating appreciable measurement repeatability.

Further to the comparison of internal versus external deployment, the PEC sensor arrangement was also validated on a pipe whose actual wall thickness ground truth (GT) had been previously obtained, with the results collected in Fig. 6. Attaining the GT is a destructive process, whereby the pipes are first exhumed, then both internal and external pipe surfaces are grit-blasted to remove rust and graphitization, the by-products of the corrosion process inflicted on a buried pipeline, leaving only the bare metal - the target of the PEC sensor measurement. Both surfaces are then reconstructed with a high-resolution 3D laser scanner and ray-tracing performed on the collocated upsampled internal and external pipe surface point clouds to derive the GT thickness maps at a resolution of 0.6 mm [7]. This high resolution GT can



(a) Pipe section and high resolution GT map. (b) Estimates against GT.
 Fig. 6: External PEC thickness estimates against GT.



(a) Solid model design. (b) Robot inspecting a pipeline.
 Fig. 7: NDT inspection robot design, and during field deployment in a pipeline.

then be downsampled to the sensor's 50 mm footprint by means of averaging so as to match the PEC sensor measurements in order to compare. RMS error of 1.29 mm was observed between external PEC measurements and GT, indicating reasonable agreement even when challenged by significant defects as evident from the testing pipe depicted in Fig. 6a, selected to better capture variability in the remaining wall thickness.

3 NDT Robot Kinematics, Locomotion and Control

The robotic NDT mapping unit was designed to allow accurate positioning of sensors internally on the pipe surface, in a robust and repeatable manner. To achieve this, a mechanism designed to self-align inside the pipe while providing circumferential and longitudinal control with a single actuation to place sensors against the pipe inner wall was developed, shown in Fig 7.

Mechanical Design Mecanum wheels were selected for the robot locomotion. In planar applications they enable holonomic robot motion as they allow control in all three degrees-of-freedom (DoF) available to the robot [8]. For this application it is only necessary to control two degrees-of-freedom, longitudinal and circumferential motion. By applying a non-standard wheel configuration it is possible to exploit the

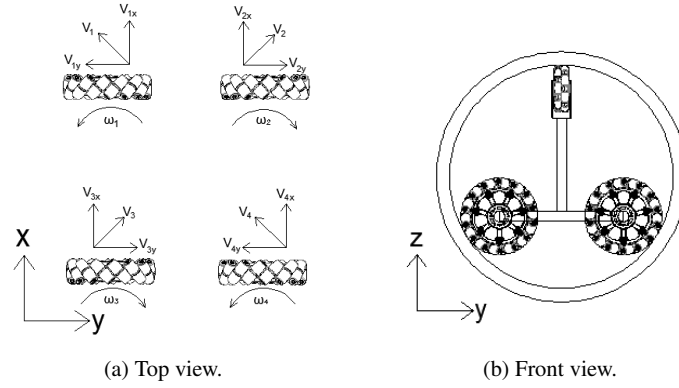


Fig. 8: Mecanum wheel layout.

unique geometry of the operating environment to passively align with the central pipe axis, automatically tracking the pipe should minor changes in direction occur. Fig. 8a & Fig. 8b demonstrate the layout designed to achieve these requirements. In this configuration, the axis of rotation of the pipe contacting rollers all pass through a single point allowing the robot to rotate freely about this point in response to an external force. When resting on a cylindrical surface, such as a pipe wall, an external restoring force is generated in response to angular disturbances which acts to return the robot to the aligned position.

Control in the longitudinal direction and rotation about the circumferential direction are achieved by controlling wheel velocities using the kinematic relations derived in Eq. 1, which follow standard forwards kinematic equations in simplified form [9], where $v_x(t)$ reflects the longitudinal velocity (m/s), $v_y(t)$ is the circumferential velocity (m/s), ω_i ($i = 1..4$) is the wheel rotation speed (rad/s) and r is the wheel radius (m).

$$\begin{aligned} v_x(t) &= (\omega_1 + \omega_2 + \omega_3 + \omega_4) \times \frac{r}{4} \\ v_y(t) &= (-\omega_1 + \omega_2 + \omega_3 - \omega_4) \times \frac{r}{4} \end{aligned} \quad (1)$$

It is essential that the angular velocities of diagonally opposite wheels are matched to prevent excessive motor loads as the robot is constrained in the z-axis. Driving each pair of diagonally opposite wheels with a single motor would achieve this requirement, however, the required drivetrain is complex and in the proposed designed control of each separate motors is implemented in software, as discussed below as part of the system overview.

To maintain stability during circumferential rotations, a set of free-wheeling omni-wheels are mounted on a parallel four bar linkage shown in Fig. 9a. This assembly is pressed against the pipe wall with a preload of approximately twice the robot weight, maintaining control authority regardless of orientation while simultaneously compensating for variation in pipe diameter. A linear actuator is included

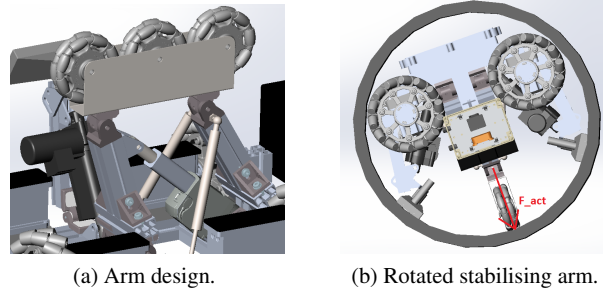


Fig. 9: Stabilising arm.

Table 1: Core component specifications.

COMPUTING	Odroid XU4 - Arm based single board computer
SENSORS	Xsens Mti-10 IMU w/ Gyro 450°/s, acc 50m/s ² Odroid USB-Cam 30FPS, FOV: 68° 3D Structure Sensor w/ HFOV: 58°, VFOV: 45°
CONTROL	Maxon Motor DCX26L, gear ratio 231:1, sensor 500 counts/turn Sensor Actuator - linear actuator, max force: 1000N Stability Actuator - linear actuator, max force: 2500N
POWER	PoE injector/splitter, 60W, 70m cable reel

to retract the omni-wheels from the pipe surface during insertion. This actuator features a spline so that it does not affect the self correcting behaviour of the parallel linkage during normal operation.

The PEC sensors are coupled to actuated lever arms using a stiff rubber joint. This joint allows the sensor to conform to the pipe surface in the presence of minor irregularities while maintaining a precise placement. The actuators drive until a stall condition is detected, allowing the sensor to be reliably placed on the pipe surface regardless of pipe variations or actuator drift.

System Overview The system uses two computers, one on-board the robot for data acquisition and actuator control, and one outside the pipe for the user interface. The entire system runs from a generator on the surface with power delivered to the robot with a power over ethernet (PoE) connection. The user interface can receive data and issue control commands in real-time over the local area network (LAN) connection provided by the ethernet tether. This approach limits operational range but provides for significantly longer operation times. To overcome power limitations of PoE, an ultracapacitor bank and bespoke charger was developed to supply bursts of high power while ensuring that the PoE equipment maintains an optimal power delivery rate. This setup provides a steady power supply for the overall system on the condition that high power maneuvers are not sustained for extended periods.

The on-board Odroid, running Linux and the Robotic Operating System (ROS), receives data from the sensor suite through a powered USB hub and controls on-board actuators via digital input/outputs pins. Each sensor has it's own monitoring node to manage incoming data and publish to the communication layer. Custom

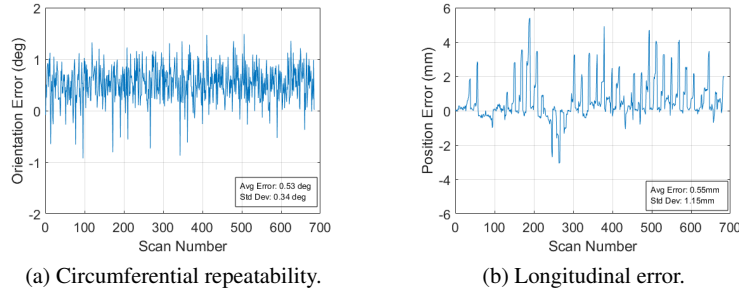


Fig. 10: Circumferential and longitudinal consistency.

task allocation/behaviour nodes then subscribe to the data streams, processing and publishing control commands as required to the motor and actuator nodes. System control is accomplished using a state machine, which allows both user and autonomous control modes for consistent data retrieval and safe user override. When switched into automatic scanning mode, the circumferential angle and longitudinal position are managed using independent set-point control loops. This simplifies both the kinematics and the algorithms required for control. Controlling circumferential angle is achieved using the on-board IMU and a standard PID control algorithm. The IMU publishes attitude data to ROS at a fixed rate of 100Hz. As each data packet is received, the attitude data is transformed into the local coordinate frame to maintain consistency even when the pipe is not level. Similarly, longitudinal control is achieved using odometry calculated using encoder readings published at a 100Hz and filtered to detect wheel stalls. In addition, an overriding human in the loop (HITL) input allows direct control of the longitudinal position. This is used to recover when odometry fails due to motor stalls or excessive wheel slip during the ring-to-ring transitions. A laser distance sensor is utilised to confirm longitudinal position when conditions are safe to deploy in the excavation pits. Details of the system are collected in Table 1

Motion Validation Consistency during automated scanning was verified at onsite trials, with angular repeatability and translational slip during rotation being the key metrics providing confidence in the sensor placement accuracy. Data was collected from an IMU to validate robot orientation, and a laser distance sensor was used to confirm longitudinal positions. Fig. 10a shows the measured rotation angle error during repeated scanning cycles of 180° using 10° increments. The observed offset of 0.53° in relation to the set-point was found to be originated by the pressing action of the sensor against the pipe wall. Fig 10b shows longitudinal drift during these scans. An average error of 0.55mm was produced (maximum 5.4mm). Since PEC sensing produces a result averaged over a 50x50mm area, and scan rings are spaced at increments of 100mm, a 5mm drift in the longitudinal direction is well within the safety margins generally assumed for failure prediction analysis in civil infrastructures. Given overall sensing and mechanical constraints, the system operates at slow speeds: deployment runtime metrics showed an average spool completion time of

166 minutes, or 1.3m/h. This includes 216 seconds of automated scanning for each ring, with 30-60 seconds dedicated to motion from one ring to the next.

4 Field Pipeline Inspection Results

The proposed robotic device has been extensively deployed in a buried 1 km live CI Cement Lined (CICL) pipeline provided by a utility in Sydney, Australia, in what effectively constitutes a unique worldwide opportunity for the advancement of NDT sensing and automation research in the field [10]. The pipeline has been decommissioned and is therefore no longer part of the utility’s live network. However a connection point to an adjacent 600 mm water main and various scour valves and hydrants allow for the pipeline to be pressurised and discharged as needed. Details of the pipeline are collected in Table 2. Pipe sections between 3 and 4 m in length were targeted for scanning by inserting the inspection robot through a removed pipe section, be that a previously replaced section, as shown in Fig. 1c, or a new cut-out. An example of an inspection plan is shown in Fig 11.

As mentioned in Section 1 the salient novelty of the proposed robotic integrity assessment is the ability to carry out internal detailed inspections that enable dense mapping where identification of the geometry of wall loss patches can be confirmed. An example of the final outcome achieved is shown in Fig. 12d, where measurements indicative of the lead run joints are also shown. To achieve this outcome various inspection patterns were studied to mitigate the slow robot examination speed reported in Section 3, and it was proven that circumferential rings 100 mm apart in axial distance were able to reconstruct detailed dense maps by means of Gaussian Process (GP) [11] spatial data dependences from limited NDT inspection data [12]. Given the 50mm sensor footprint this effectively meant skipping every other ring with considerable time savings yet inconsequential information loss in relation to map quality and sizing of critical patches.

Robot localisation with respect to an entry point while travelling towards a section targeted for inspection was done by means of robot odometry, measurement of tether release and accounting for spool joints traversed as seen by the robot camera. Validation from an external laser scanner mounted at the entry point as seen

Table 2: Test-bed specifications, adapted from [10].

Year Installed	1922
Nominal Pipe Diameter	600 mm
Internal Pipe Diameter	579 mm to 590 mm (with cement lining)
External Pipe Diameter	662 mm to 666 mm
Nominal Wall Thickness	27 mm
Material	Pit Cast Iron
Internal Liner	Cement (installed in 1964)
Cement Lining Thickness	9.5 mm to 16.5 mm

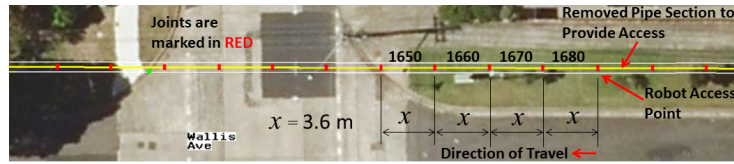


Fig. 11: A typical inspection plan.

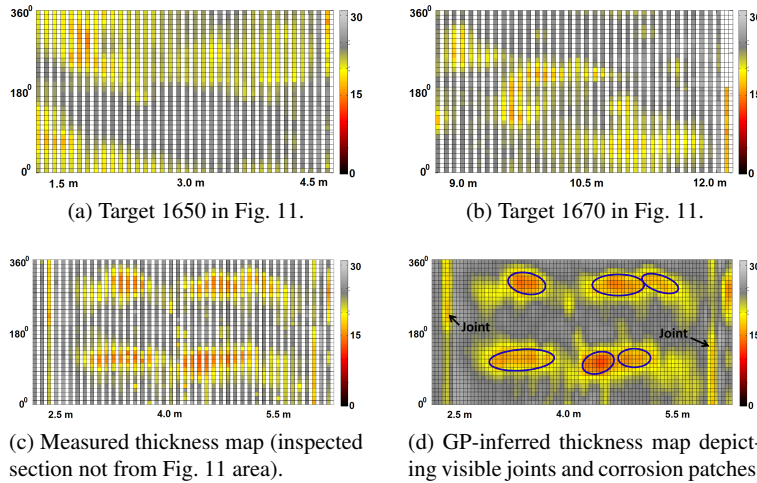


Fig. 12: Various examples of remaining pipe wall thickness maps as measured by the robotic wall inspection during field deployment on buried critical water mains.

in Fig was also used when it was deemed safe to be deployed in the field excavation pit. Moreover, discontinuity on spool joints also reveals a characteristic PEC signal comparable to a crack that was also exploited in case of ambiguity about spool length. After reaching the target spool, circumferential and longitudinal ring inspections were undertaken as described in Section 3 to generate maps such as those depicted in Fig. 12. Where wall loss is present the spread of the reduction is clearly evident and can be identified and measured. Such patches are modelled as ellipses (see Fig. 12d), and their defining parameters can then be incorporated for stress calculation and remaining life prediction of the asset [1].

Prior to using the robotic tool for extensive measurements, repeatability tests were also carried out on pipe sections at the test-bed to ascertain the performance of the robotic inspection unit in-situ. Results from one of the tests are shown in Fig. 13. The error histogram in Fig. 13c suggests a close to zero-mean Gaussian (0.112 mm mean, 0.869 mm standard deviation). Information such as minimum, maximum and average thickness of the inspected pipe section are key parameters of interest to water utilities for stress analysis and asset management in general. Table 13d collects the most typical quantitative information being currently reported with the robotic device on the two inspections shown - Map A (Fig. 13a) and Map B (Fig. 13b).

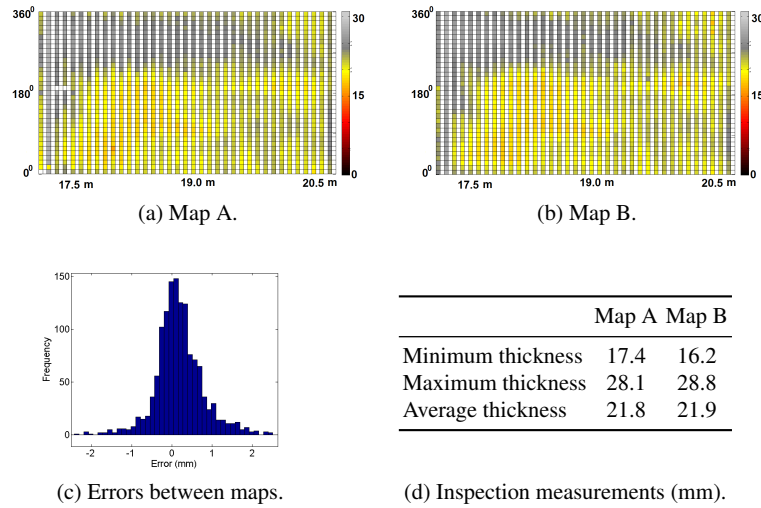
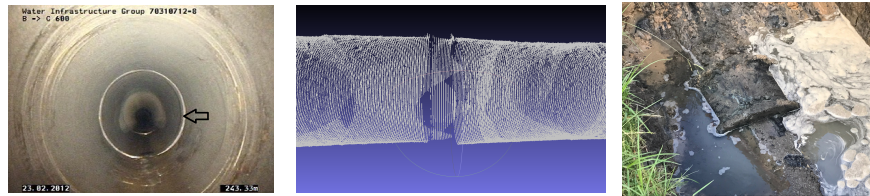


Fig. 13: Robotic inspection repeatability tests on a single pipe section.



(a) Picture of anomalous narrowing (white ring at pointer). (b) 3D reconstruction of anomaly captured by RGBD robot sensor. (c) Outer clamp found after excavation.

Fig. 14: Uncharted pipe anomaly found during inspection; verification excavation.

Pipe Inner Surface Profiling In addition to PEC measurements, perceptual information from video streaming and point clouds of the pipe inner surface (cement lining) can also be recorded with the RGB camera and the 3D structure sensor mounted at the front of the robot. The latter in particular allows mapping the geometry of the pipe inner surface in order to evaluate the surface unevenness, variation in the nominal pipe diameter and mapping the structure of in-pipe features (chainage, off-takes, valves). Moreover, reconstructing the inner surface profile has the advantage that it enables identifying and locating uncharted coarse anomalies present on the cement lining surface which may impede motion of ILI tools. An example of the latter was apparent during one of the inspections where the robot encountered an abnormality in the form of pipe narrowing during the experiment is shown in Fig. 14b. The mean diameter of the narrow region was observed to be 579 mm while the expected nominal diameter of the cement lined inner surface is expected to be close to 600 mm. A posterior excavation found an uncharted outer clamp, shown in Fig 14c, whose existence was not known to the utility.

5 Concluding Remarks

An in-line robotic solution for the inspection of buried critical water mains and its evaluation during field deployments has been presented in this paper. A singular kinematic locomotion design that optimizes mobility in such tubular environments has been coupled with an embedded NDT sensing solution based on PEC for measurements unsusceptible to sensor lift-off, as typically found in cement lined water pipelines. The device addresses a utility sector need for an automatic NDT inspection vehicle that can report dense pipe wall thickness discrimination as prescribed by failure prediction analysis, and that can be deployed in an opportunistic manner - e.g. when a mains break occurs, or during valve inspection or repair programs when pipelines are discharged and access made available. Extensive results have proven the validity of the solution on laboratory tests and field pipeline inspections which demonstrate the feasibility of the device and sensing configuration to provide meaningful 2.5D geometric maps.

References

1. J. Ji, D. Robert, C. Zhang, D. Zhang, J. Kodikara, Probabilistic physical modelling of corroded cast iron pipes for lifetime prediction, *Structural Safety* 64 (2017) 62–75.
2. Z. Liu, Y. Kleiner, State of the art review of inspection technologies for condition assessment of water pipes, *Measurement* 46 (1) (2013) 1–15.
3. C. Huang, W. Xinjun, X. Zhiyuan, Y. Kang, Pulsed eddy current signal processing method for signal denoising in ferromagnetic plate testing, *NDT & E International* 43 (7) (2010) 648–653.
4. Z. Xu, X. Wu, J. Li, Y. Kang, Assessment of wall thinning in insulated ferromagnetic pipes using the time-to-peak of differential pulsed eddy-current testing signals, *NDT & E International* 51 (2012) 24–29.
5. C. Huang, X. Wu, An improved ferromagnetic material pulsed eddy current testing signal processing method based on numerical cumulative integration, *NDT & E International* 69 (2015) 35–39.
6. N. Ulapane, A. Alempijevic, T. Vidal-Calleja, J. V. Miro, J. Rudd, M. Roubal, Gaussian process for interpreting pulsed eddy current signals for ferromagnetic pipe profiling, in: *Conference on Industrial Electronics and Applications*, 2014, pp. 1762–1767.
7. B. Skinner, T. Vidal-Calleja, J. V. Miro, F. De Bruijn, R. Falque, 3D point cloud upsampling for accurate reconstruction of dense 2.5D thickness maps, in: *Australasian Conference on Robotics and Automation*, 2014, p. 7.
8. L. Xie, C. Scheifele, W. Xu, K. A. Stol, Heavy-duty omni-directional mecanum-wheeled robot for autonomous navigation: System development and simulation realization, in: *International Conference on Mechatronics*, IEEE, 2015, pp. 256–261.
9. H. Taheri, B. Qiao, N. Ghaeminezhad, Kinematic model of a four mecanum wheeled mobile robot, *International Journal of Computer Applications* 113 (2015) 6–9.
10. J. V. Miro, J. Rajalingam, T. Vidal-Calleja, F. de Bruijn, R. Wood, D. Vitanage, N. Ulapane, B. Wijerathna, D. Su, A live test-bed for the advancement of condition assessment and failure prediction research on critical pipes, *Water Asset Management Intl.* 10 (2) (2014) 3–8.
11. C. E. Rasmussen, C. K. Williams, *Gaussian processes for machine learning*. 2006, The MIT Press, Cambridge, MA, USA.
12. L. Shi, J. V. Miro, Towards optimized and reconstructable sampling inspection of pipe integrity for improved efficiency of NDT, in: *World Water Congress, IWA*, 2016, p. 8.